Title

U-Pb ages of detrital and volcanic zircons of the Toro Negro Formation, northwestern Argentina: Age, provenance and sedimentation rates

Authors

Amidon, William H
Ciccioli, Patricia L
Marenssi, Sergio A
et al.

Publication Date

2016-10-01

DOI

10.1016/j.jsames.2016.05.013

Peer reviewed

Journal of South American Earth Sciences 70 (2016) 237–250

Contents lists available at ScienceDirect

Journal of South American Earth Sciences

journal homepage: www.elsevier.com/locate/jsames

U-Pb ages of detrital and volcanic zircons of the Toro Negro Formation, northwestern Argentina: Age, provenance and sedimentation rates

William H. Amidon [a, *], Patricia L. Ciccioli [b], Sergio A. Marenssi [b], Carlos O. Limarino [b], G. Burch Fisher [c, d], Douglas W. Burbank [d], Andrew Kylander-Clark [d]

[a] Geology Department, Middlebury College, Middlebury, VT, 05753, USA
[b] Departamento de Ciencias Geológicas, IGeBA, Facultad de Ciencias Exactas y Naturales, Universidad de Buenos Aires-CONICET. Pabellón 2, 1° piso, Ciudad Universitaria, C1428EHA Buenos Aires, Argentina
[c] Jackson School of Geosciences, University of Texas at Austin, Austin, TX, 78712, USA
[d] Earth Research Institute, University of California, Santa Barbara, CA, 93106, USA

ARTICLE INFO

Article history:
Received 13 November 2015
Received in revised form
23 May 2016
Accepted 26 May 2016
Available online 28 May 2016

Keywords:
Tephra
Vinchina
Fiambala
Bermejo
Famatina
U-Pb
Zircon
Precordillera
Valle Fertil

ABSTRACT

The Toro Negro Formation is a foreland sequence in western La Rioja province, Argentina, which records the late-stage tectonic evolution of the Vinchina Basin. Together with the underlying Vinchina Formation, these two units represent one of the thickest and longest continually exposed foreland sections in northwest Argentina. The Vinchina basin is uniquely situated between the Toro Negro and Umango blocks of the Western Sierra Pampeanas to the north and south, the Precordillera to the west, and the Sierra de Famatina to the east. New U-Pb dating of volcanic tephra provides improved age constraints on the pace of sedimentation, and U-Pb ages of detrital zircons serve to strengthen existing provenance interpretations. We show that deposition of the Toro Negro Formation spans roughly 6.9 to 2.3 Ma: Late Miocene to Early Pleistocene. A high-relief, erosional unconformity with the underlying Vinchina Formation developed sometime between 9.3 and 6.9 Ma, although stratigraphic considerations suggest it spanned only the later part of this time interval (perhaps 7.5–6.9 Ma). Above this unconformity, undecompacted sedimentation rates are remarkably high at ~1.2 mm/yr, slowing to ~0.3 mm/yr after ~6 Ma. An unconformity in the upper part of the section is constrained to occur sometime between 5.0 and 3.0 Ma, probably beginning not long after 5.0 Ma. The timing of both unconformities broadly Matches the timing of inferred tectonic events in the Sierra Famatina ~50 km to the east, the Fiambalá basin to the north, and the Bermejo basin to the south, suggesting they May record regional tectonism at these times. Provenance interpretations of detrital zircon spectra are consistent with previous interpretations based on sediment petrography. They show that provenance did not change significantly during the course of Toro Negro deposition, precluding major tectonically-induced drainage reorganization events. Sediments were derived primarily from the north (Toro Negro Block) and west (Precordillera). The data are consistent with a subtle increase in sediment supply from the Precordillera beginning around 6.5 Ma.

1. Introduction

Foreland basin sediments are important recorders of the tectonic and climatic evolution of mountain ranges. Such stratigraphic successions have proven especially useful in unraveling the tectonic evolution of the eastern Andes, where the structural style changes rapidly and precise age control is commonly available from tephrochronology. For example, foreland sequences in northern Argentina have been critical to distinguishing regions of in-sequence thrust progradation, such as the Subandean belt, from regions of out-of-sequence thrusting that are more characteristic of the Sierras Pampeanas and Santa Barbara System (Strecker et al., 2007). Foreland sediments are also valuable records of terrestrial climate and vegetation, presenting an additional impetus for understanding their age, provenance, and depositional setting (e.g. Mulch et al., 2010).

The Bermejo basin of NW Argentina is a world-class example of

* Corresponding author.
E-mail address: wamidon@middlebury.edu (W.H. Amidon).

http://dx.doi.org/10.1016/j.jsames.2016.05.013
0895-9811/

a foreland basin that has evolved by a mixture of thin- and thick-skinned deformation (Beer and Jordan, 1989; Collo et al., 2011; Jordan et al., 1993, 2001; Milana et al., 2003). The classic model of Jordan et al. (2001) involves a transition from an initially "simple foreland" that is subsequently divided into sub-basins by the rise of mountain ranges along deep-seated basement thrusts to create a "broken foreland". In this model, the simple foreland stage from (~20-8 Ma) is primarily a flexural response to shortening in the Frontal Cordillera and Precordillera to the west. By ~6.5 Ma, uplift of the Sierras Pampeanas fragments the Bermejo foreland into more localized depocenters (Jordan et al., 2001). As additional studies have focused on these localized depocenters, it has become clear that some of the basement uplifts, particularly those in the north, such as the Vinchina Basin, are older and record a complex interplay of thin- and thick-skinned deformation throughout the Miocene (e.g. Dávila and Astini, 2007; Ciccioli et al., 2011, 2013a; Marenssi et al., 2015). Thus, many questions remain about the precise spatio-temporal pattern with which the broken foreland evolved, and how it was controlled by pre-existing structures and changes in the Pacific-South America plate dynamics.

This study seeks to better understand the history of the Toro Negro Formation, a clastic foreland sequence deposited in the Vinchina depocenter (the modern Bolson de Jagüé basin) at the northern end of the Bermejo Basin near 28.5 °S (Fig. 1). The Vinchina basin is a classic example of a localized depocenter, because it is bounded to the north, south, and east by basement-cored uplifts (Fig. 2). The Toro Negro block to the north and the Umango-Espinal arch to the south are both part of the Western Sierras Pampeanas, whereas the Sierra de Famatina to the east and Sierra de Narváez to the northeast are part of the Famatina System. To the west, the Vinchina depocenter is bound by the Frontal Cordillera and the northernmost extent of the Precordillera (Figs. 1 and 2). The Frontal Cordillera is composed of metamorphic basement, Late Paleozoic to Triassic granitoids, and young Cenozoic volcanics (Caminos, 1972; Caminos et al., 1979; Caminos and Fauqué, 2001). Farther east, the Precordillera is a thin-skinned fold-and-thrust belt, creating a series of north-south oriented mountain ranges immediately west of the Jagüé basin. The Vinchina depocenter also sits ~50 km north of a major basement structural lineament known as the Valle Fértil lineament, which is interpreted to be an important basement structure whose Miocene reactivation exerted a strong control on partitioning of the Bermejo Basin (Ciccioli et al., 2011, 2013a). The Toro Negro Formation is thus well situated to record both uplift of basement blocks in the Western Sierras Pampeanas, as well as thrust activity in the northern Precordillera (Ciccioli, 2008; Ciccioli et al., 2014a).

The sedimentology of the Vinchina depocenter has been well studied over the past 10 years (e.g. Tripaldi et al., 2001; Limarino et al., 2001; Ciccioli, 2008; Ciccioli and Marenssi, 2012; Ciccioli et al., 2011, 2013b, 2014a; Marenssi et al., 2015). In particular, the modal composition of sandstones and conglomerates has proven an effective means to establish source areas and to explore the relation between shifts in compositional framework and changes in watershed configuration (Ciccioli, 2008; Ciccioli et al., 2014a). Sandstone composition does not, however, depend exclusively on the source rocks: it may be affected by the physiography and chemical weathering in the source area, by reworking and abrasion of the sediments during transportation and sedimentation, by recycling of older sediments, and by diagenetic effects (Amorosi and Zuffa, 2011; Dickinson and Suczek, 1979; Espejo and López-Gamundí, 1994). Additionally, uncertainty regarding the age of the Toro Negro Formation has prevented sedimentological observations from being interpreted in a well-dated regional framework. Age estimates for the Toro Negro Formation have ranged from Plio-Pleistocene (Reynolds, 1987; Tabbutt et al., 1989; Ré and Barredo, 1993) to late Miocene-early Pliocene (Ciccioli et al., 2005; Collo et al., 2011). In the absence of better time control, significant uncertainty persists concerning the timing and pace of Toro Negro deposition.

This study presents eight, new U/Pb zircon ages on volcanic tephra from the La Troya section. These new dates refine the age of the Toro Negro Formation to approximately 6.87 to 2.37 Ma (Late Miocene-earliest Pleistocene). We also combine existing petrographic and clast-count data with U-Pb dating of detrital zircons from eight sites to better constrain provenance changes. These results demonstrate that the Toro Negro Formation is somewhat younger than previously thought, they define four-fold changes in sediment-accumulation rates, and they support the conclusions of Ciccioli et al. (2014a) that these sediments are derived primarily from the north and west with only minor changes in provenance over time.

2. Geologic setting

The bedrock geology in the study area is a mosaic of accreted terranes intruded by igneous rocks that record nearly every stage of Andean margin evolution. The geologic evolution is briefly reviewed here to provide a context for interpretation of detrital U-Pb ages. During Grenville time (~1300–1050 Ma), the margin of the Rio de la Plata craton was sutured with Laurentia as part of the supercontinent Rodinia (Ramos and Folguera, 2009). Numerous granitoids were intruded and sedimentary rocks accreted, which are now preserved as high-grade schists and gneisses exposed in basement blocks throughout the Western Sierras Pampeanas, e.g., the Maz, Espinal, and Umango ranges(Casquet et al., 2008; Colombo et al., 2009; Martina et al., 2005; Ramos and Folguera, 2009; Rapela et al., 2010). Spatially significant meta-sedimentary units include the dominantly quartz schists and gneisses of the El Espinal and Tambillito Formations (Turner, 1964), and the dominantly pellitic schists and gneisses of the Sierra de Maz, El Zaino, and El Taco Groups (Kilmurray, 1971).

By the early Cambrian (~535 Ma), a subduction margin was established, followed shortly by accretion of the Pampia Terrane during the middle Cambrian. Granitoids and meta-sedimentary rocks of this age are widely exposed in the Eastern Sierras Pampeanas, but are less common near the study area (Pankhurst et al., 1998). Subduction was reestablished by the early Ordovician accompanied by voluminous plutonism and intrusion of the Famatina granitoid belt from ~465 to 490 Ma and by compression during the ensuing Ocloyic orogeny (Pankhurst et al., 1998; Rapela et al., 1998; Rubiolo et al., 2002). Famatinian granites are widely exposed in the Sierra de Famatina and Sierra de Narváez (Famatina System), and sparsely exposed in the Sierra de Umango (Western Sierras Pampeanas), with ages from~ 464-481 Ma (Pankhurst et al., 2000; Rapela et al., 1999; Rubiolo et al., 2002; Varela et al., 2000, 2011). Ordovician Famatinian arc volcanism was accompanied by deposition of siliciclastic and volcaniclastic sedimentary rocks in a back-arc basin (Bahlburg and Herve, 1997; Sims et al., 1998). A thick (~3200 m) succession of Ordovician sediments exposed in the Famatina System includes siliciclastic, rocks such as the Negro Peinado, Suri, Las Planchadas, Río Bonete, Achival, La Escondida, Aguadita, and Bordo Atravesado Formations (Aceñolaza and Toselli, 1981; Aceñolaza et al., 1996; Astini et al., 2003; Mangano and Droser, 2003; Turner, 1967; among others).

During the latest Ordovician and Silurian, the Precordillera (Cuyania) Terrane docked and sutured a crustal fragment with an overlying shelf sedimentary sequence during the Ocloyic orogeny (Ramos et al., 1986; Rapela et al., 1998). The strictly defined Cambro-Ordovician Precordillera terrane is exposed to the south of the Vinchina region, including the Las Vacas, Trapiche, Yerba Loca,

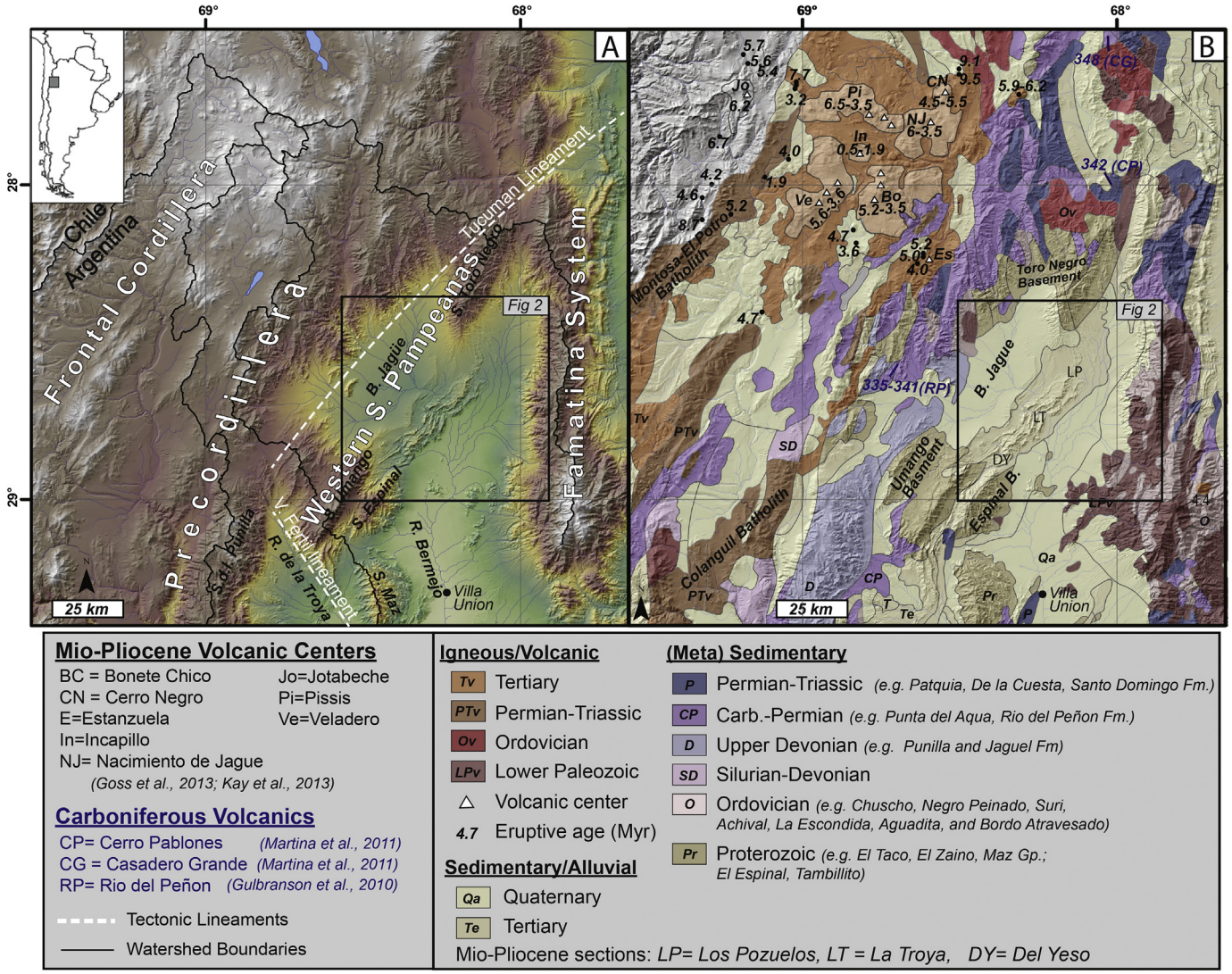

Mio-Pliocene Volcanic Centers

BC = Bonete Chico
CN = Cerro Negro
E=Estanzuela
In=Incapillo
NJ= Nacimiento de Jague
Jo=Jotabeche
Pi=Pissis
Ve=Veladero
(Goss et al., 2013; Kay et al., 2013)

Carboniferous Volcanics

CP= Cerro Pablones *(Martina et al., 2011)*
CG = Casadero Grande *(Martina et al., 2011)*
RP= Rio del Peñon *(Gulbranson et al., 2010)*

Tectonic Lineaments
Watershed Boundaries

Igneous/Volcanic

Tv Tertiary
PTv Permian-Triassic
Ov Ordovician
LPv Lower Paleozoic
△ Volcanic center
4.7 Eruptive age (Myr)

Sedimentary/Alluvial

Qa Quaternary
Te Tertiary

(Meta) Sedimentary

P Permian-Triassic *(e.g. Patquia, De la Cuesta, Santo Domingo Fm.)*
CP Carb.-Permian *(e.g. Punta del Aqua, Rio del Peñon Fm.)*
D Upper Devonian *(e.g. Punilla and Jaguel Fm)*
SD Silurian-Devonian
O Ordovician *(e.g. Chuscho, Negro Peinado, Suri, Achival, La Escondida, Aguadita, and Bordo Atravesado)*
Pr Proterozoic *(e.g. El Taco, El Zaino, Maz Gp.; El Espinal, Tambillito)*

Mio-Pliocene sections: *LP= Los Pozuelos, LT = La Troya, DY= Del Yeso*

Fig. 1. Left panel: shaded relief image of the study area with major physiographic provinces labeled and watershed boundaries shown in black. The Western Sierras Pampeanas includes the major basement uplifts that surround the Jagüé Basin (Toro Negro, Maz, Espinal, and Umango). The Famatina System bounds the basin on the east. Right panel: 1:1,000,000 scale geologic map provided by El Servicio Geológico Minero Argentino (SEGEMAR). White triangles denote summits of major volcanic centers, black dots show the locations of geochronologic ages, and numbers denote their ages in Myr (Goss et al., 2013; Kay et al., 2013). Age ranges are given for the major volcanic centers whose extent is outlined in light orange. CG, CP, and RP denote recently dated Carboniferous volcanigenic deposits.

and many other formations (Fig. 7). However, we use the broader term of Precordillera to refer to the thin-skinned fold-and-thrust belts exposed immediately west of our field area, which includes the Ordovician Chuscho and Rio Bonete formations overlain by the younger Carboniferous-Permian formations described below (Fig. 2).

After Cambro-Ordovician thickening, significant topography likely characterized the western margin of South America. The late Paleozoic was characterized by sedimentation into basins flanking this topography, including the Río Blanco Basin in our study area(Limarino et al., 2006; López Gamundí, 1987; Scalabrini Ortiz, 1973). Associated sedimentary units include the latest Devonian Jagüél and Punilla Formations, which are unconformably overlain by the Carboniferous Punta del Agua and Río del Peñón Formations (Gulbranson et al., 2010, 2015; Henry et al., 2008; Net and Limarino, 2006). Sparsely preserved early Permian clastic sequences are also present, including the Patquia/De la Cuesta Formations (Caselli and Limarino, 2002). Volcanism continued into the Early Carboniferous, as evidenced by granites, such as the Potrerillos and Las Tunas Plutons exposed immediately west of the Jagüé Basin (Dahlquist et al., 2006; Grosse et al., 2009; Rapela et al., 1982; Varela et al., 2011). Early Carboniferous rhyolite and andesite intervals (335–348 Ma) are also exposed in the north and west of the study area, some of which were initially mapped as Ordovician (Gulbranson et al., 2010; Martina et al., 2011).

By mid-Permian time, widespread subduction and arc volcanism were again affecting the region, as recorded by at least two classes of igneous rocks. First, arc-type granitoids were intruded, often referred to as the Frontal Cordillera Plutons or Elqui Complex, and have been dated to ~267–254 Ma (Llambías and Sato, 1992; Nasi et al., 1985). The Colangüil batholith is the largest intrusion of this age in the study area, exposed about 100 km to the southwest. A second phase of plutonism is recorded by the batholiths of the Ingaguas Complex, which were emplaced from ~260 to 192 Ma and are exposed in Montosa-El Potro batholith ~150 km to the northwest, well outside of the modern watershed (Mpodozis and Kay, 1992). These rocks are roughly equivalent to the Choiyoi plutons that are widely exposed between ~30 and 34° S.

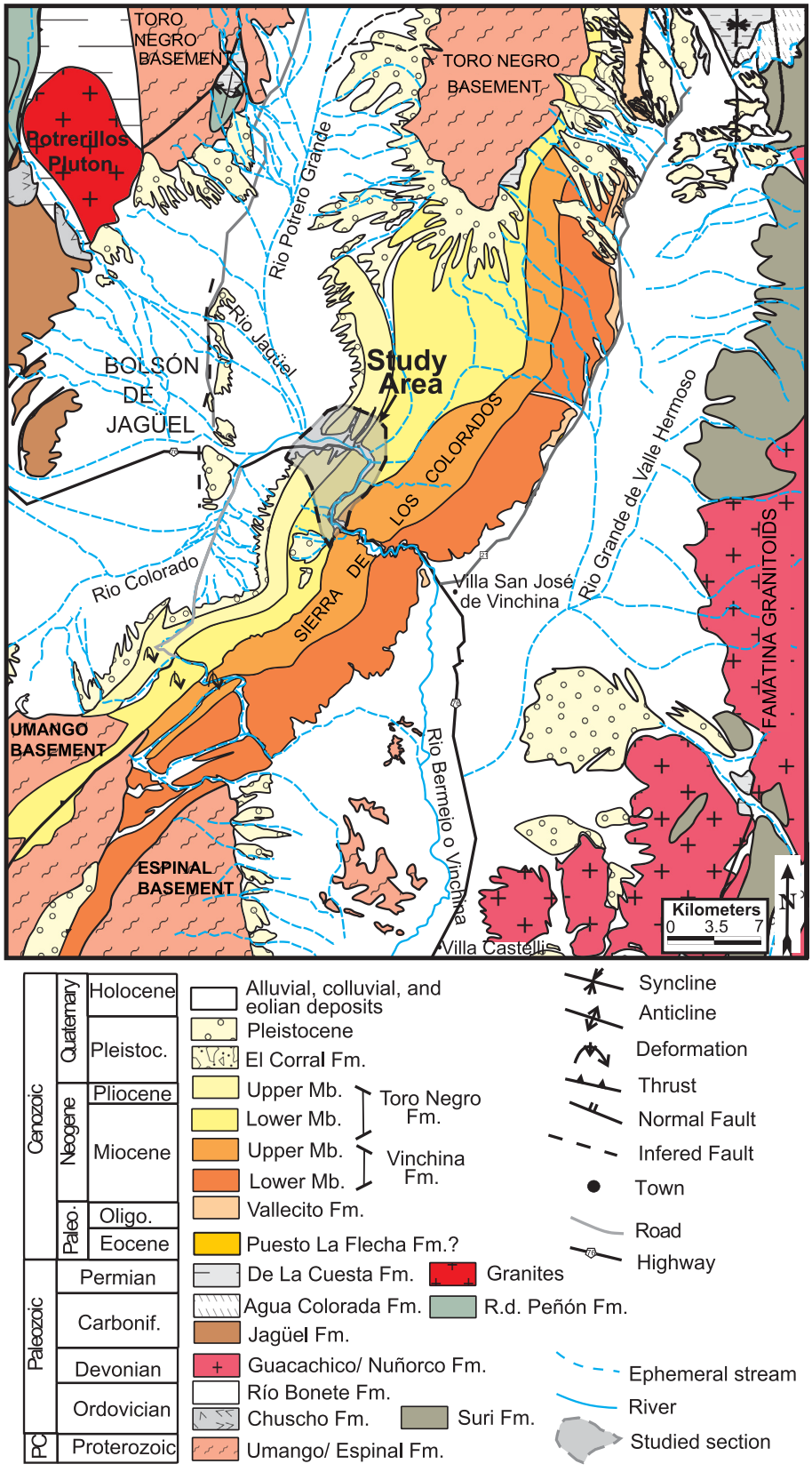

Fig. 2. Detailed Geological map of the study area including regional stratigraphy as discussed in section 2 of the text. Modified from Ciccioli (2008).

During the Mesozoic, scarce volcanism and continental sedimentation took place to the west and south of the study area as recorded in the Santo Domingo and Ciénaga de Río Huaco Formations (Caminos et al., 1995; Coughlin, 2000; Caminos and Fauqué, 2001; Limarino et al., 2005; Tedesco et al., 2007). These extensional depocenters were developed due the breakup of Gondwana along previous basement lineaments in the northwest of Argentina.

Throughout much of the Cenozoic, the region existed as a relatively quiescent retro-arc environment to the east of the main volcanic axis. As the Andean orogeny got underway at about 20 Ma, significant shortening was accommodated in the Frontal Cordillera and Precordillera, causing development of the Bermejo Basin (Jordan et al., 2001). By about 20 Ma, flat-slab subduction was initiated (Kay et al., 1987), and by 10 Ma, flat-slab subduction began affecting the eastern Andes between the latitudes of ~27–33 °S (Jordan et al., 1983). This low-dip subduction largely extinguished volcanism to the south of the study area (Kay and Abbruzzi, 1996), and ultimately accelerated deformation. Because the study area sits at the transition from flat-slab subduction (south) to regular subduction (north), late Cenozoic volcanics are abundant to the northwest of the study area, but sparse to the southwest (Goss et al., , 2013; Kay et al., 2013) (Fig. 1B).

3. Previous work

3.1. Stratigraphy of the Vinchina depocenter

At least four major Upper Paleogene and Neogene formations have been deposited in the Vinchina depocenter: the Vallecito, Vinchina, Toro Negro, and El Corral (Fig. 2). In the La Troya depocenter to the south of the study area, the pre-Miocene Puesto la Flecha and Vallecito formations have a combined thickness of ~1100 m and are composed of lacustrine facies and cross-bedded eolian sandstones, respectively (Borrello and Cuerda, 1967; de la Fuente et al., 2003; Tripaldi and Limarino, 2005).

The rapidly deposited Miocene Vinchina Formation is ~5100 m thick and is composed mostly of reddish sandstones and shales deposited in fluvial and lacustrine environments (Ramos, 1970; Turner, 1964; Tripaldi et al., 2001). Recent U-Pb ages estimate the formation to span roughly 15.6–9.2 Ma (Ciccioli et al., 2014b; Collo et al., 2011). The fluvial sandstones of the Lower Member of the Vinchina Formation are interpreted to herald the initiation of uplift in the Sierra Espinal/Maz arch and the Sierra del Toro Negro, due to the interplay of two transpressional faults: the Tucuman and Valle Fertil lineaments (Fig. 1A)(Cobbold et al., 1993; Ciccioli et al., 2011; Rossello et al., 1996). This interpretation is supported by the onset of underfilled basin conditions and the appearance of abundant microcline sourced from the high-grade basement rocks (Tripaldi et al., 2001). However, the details of fault reactivation around the Vinchina basin remain somewhat unclear. Apatite fission-track ages from the Sierra de Maz show uplift and cooling synchronous with Vinchina deposition (15–10 Ma), whereas ages from the Valle Fertil hanging wall (~200 km south) suggest the main period of reactivation occurred later between ~10 and 5 Ma (Coughlin et al., 1998). The Upper Member of the Vinchina Formation was deposited in a more isolated basin that formed as continued uplift of the Espinal and Maz blocks separated the Vinchina depocenter from the La Troya depocenter immediately to the south (Ciccioli et al., 2011).

The overlying Toro Negro Formation (~2500 m thick, Turner, 1964) is divided into an upper and lower member (Ramos, 1970), further subdivided into three depositional sequences, I, II, and III, which are henceforth referred to as DSI, DSII, and DSIII (Ciccioli et al., 2014a). The Upper Member is equivalent to DSIII and the Lower Member is split between DSI and II (Fig. 3). The top and bottom of all DS units are demarcated by erosional unconformities, which may record periods of regional base-level change (Turner, 1964; Ramos, 1970; Ciccioli, 2008; Ciccioli and Marenssi, 2012; Ciccioli et al., 2014a). The basal unconformity of DSI has the highest relief, including a paleo-valley carved into the underlying Vinchina Formation, which causes DSI to be ~25% thicker (roughly 1000 m) in the north, where it fills the valley (Limarino et al., 2010). This basal unconformity and the anastomosing and braided incised channels overlying it suggest DSI records the onset of a transpressional foreland (Ciccioli et al., 2013a). DSII and III become considerably coarser in the La Troya section and record unconfined alluvial gravels prograding across a filled basin (Ciccioli, 2008; Ciccioli and Marenssi, 2012). DSIII is composed of thick successions of clast-supported conglomerates and coarse sandstones interpreted to have been deposited in piedmont and proximal braided plains; these strata alternate with comparatively thin intervals dominated by mudstones, fine-grained tuffs, and tuffaceous deposits (Ciccioli, 2008; Ciccioli and Marenssi, 2012).

Finally, the El Corral Formation, comprising breccias, conglomerates, and coarse sandstones, appears to have been deposited in alluvial fans and piedmont systems. This unit records a relatively recent phase of orogenic uplift when regional foreland units were themselves uplifted and eroded (Ciccioli et al., 2011).

3.2. Provenance of the Toro Negro formation

Ciccioli et al. (2014a) combine sandstone petrofacies, conglomerate lithic identification, and paleocurrent analysis to show that sediments in the Toro Negro Formation are primarily derived from the north (Toro Negro Range), with periods of increased contribution from the west (Frontal Cordillera and Precordillera). For example, DSII shows notable north-south facies changes from fluvial conglomerates and coarse-grained sandstones in the north (Los Pozuelos section) to fine-grained successions deposited in a playa lake in the south (Del Yeso section). Preserved strata do not record material derived from the east (Sierra de Famatina) or south (Sierra de Umango). Although overall provenance changes are minor, subtle changes in provenance are summarized here and in Fig. 3.

The Toro Negro sandstones can be divided into three sandstone petrofacies: *plutonic-metamorphic, volcanic* and *mixed*. The *plutonic-metamorphic* petrofacies (PMP) is defined by (K-feldspar/plagioclase) > 1, (high-grade metamorphic lithics/volcanic lithics) > 1, and >60% of clasts derived from crystalline rocks. The *volcanic* petrofacies (VP) is defined by > 60% of volcanic components and a (K-feldspar/plagioclase) < 1. Finally, the *mixed* petrofacies(MP) shows a variable (K-feldspar/plagioclase) ratio and a relative decrease in volcanic groundmasses, quartz and crystalline rock clasts in relation to the PMP.

The lower beds of DSI are dominated by the plutonic-metamorphic petrofacies, grading upward into the mixed petrofacies towards the top of DSI (Fig. 3). Conglomerate clasts support this succession, showing a predominance of high-grade metamorphic basement clasts near the base of DSI, with secondary amounts of volcanic and sedimentary clasts and a lack of slates and phyllites (Ciccioli et al., 2014a). This composition suggests material derived primarily from basement exposures of the Western Sierras Pampeanas, most likely the Toro Negro Range, based on north-south paleocurrents and the decrease of grain size toward the south (Ciccioli, 2008; Ciccioli and Marenssi, 2012; Ciccioli et al., 2014a).

The lower part of the DSII returns to the plutonic-metamorphic petrofacies (Fig. 3) based on abundant schist, gneiss and metavolcanic fragments, as well as different types of simplectites (Ciccioli et al., 2014a). Towards the top of DSII, a shift back towards mixed petrofacies is revealed by the increased abundance of

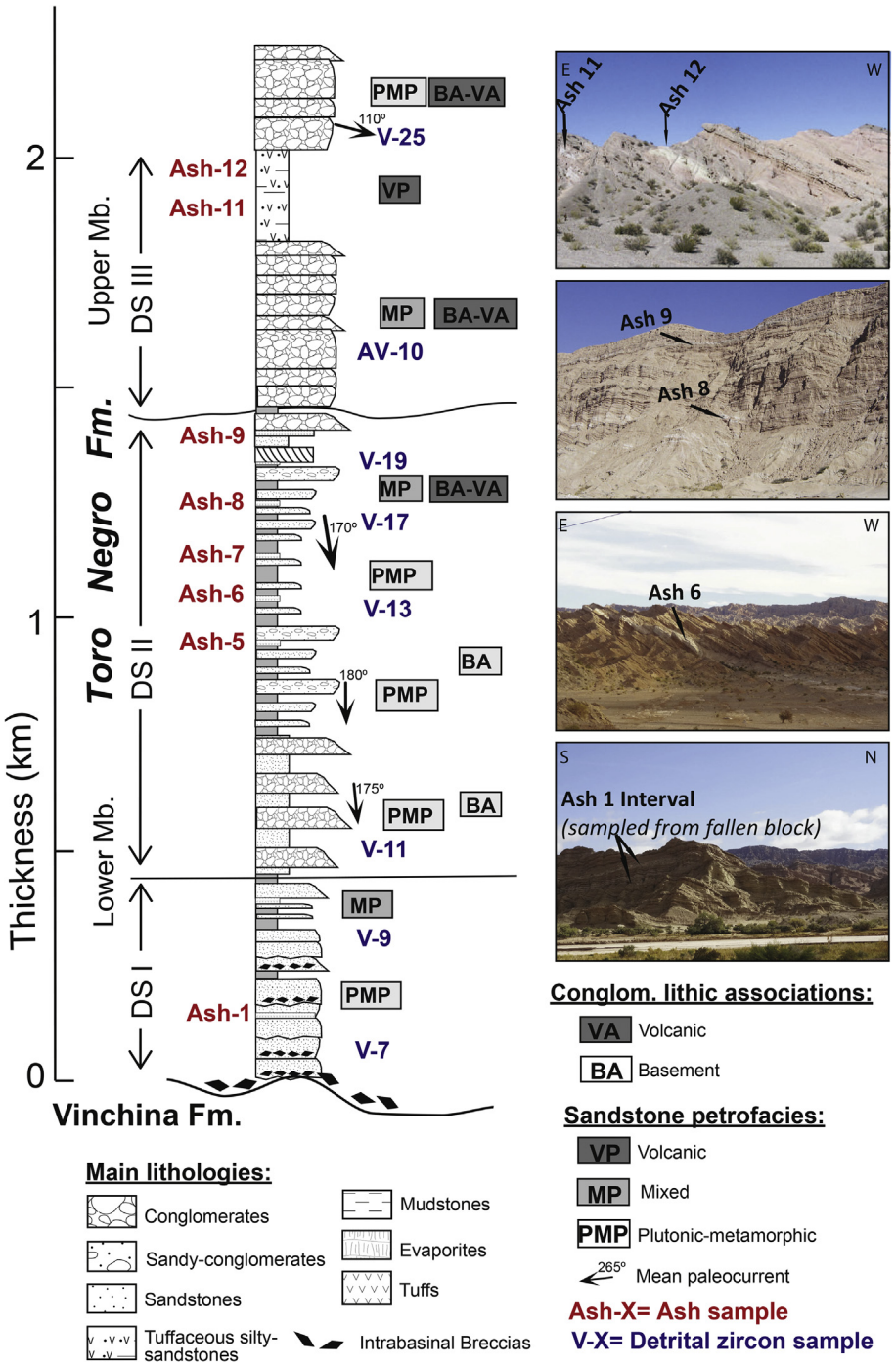

Fig. 3. Stratigraphic column showing tephra and detrital zircon samples in the context of the stratigraphy published by Ciccioli et al. (2014a). Photos at right show tephra layers sampled for U-Pb dating. They are coherent and well preserved within dominantly fluvial strata.

volcanic components. Conglomerate clasts at the top of DSII also show an increase in volcanic and sedimentary components. This increase in volcanic components towards the top of DSII suggests an enhanced sediment supply from Silurian-Carboniferous volcanic rocks of the Precordillera, perhaps combined with Cenozoic volcanic rocks of the Frontal Cordillera (Ciccioli et al., 2014a).

The lower part of DSIII is characterized by a mixed sandstone petrofacies (Fig. 3) associated with a predominance of high-grade crystalline clasts, with secondary sedimentary, volcanic, and low-grade metamorphic clasts (Ciccioli et al., 2014a). This composition suggests a persistent source of basement rocks from the Toro Negro Range to the north, with secondary contributions from the west (Ciccioli et al., 2014a). In middle DSIII, this petrofacies transitions upward to a volcanic assemblage due to the addition of intrabasinal glassy volcanic sand components, suggesting a growing neo-volcanic source to the northwest during this time. The existence of young volcanics in the headwaters is supported by the occurrence of two thick tephra beds in this part of the section, and numerous eruptive centers of this age (Figs. 1 and 3). The uppermost DSIII is marked by a shift back to plutonic-

metamorphic petrofacies due to an increase in high-grade crystalline lithics coupled with sedimentary, slate, and phyllite fragments (Ciccioli et al., 2014a). Conglomerate clasts show a similar trend; sedimentary and low-grade metamorphic clasts also become more abundant towards the middle and top of DSIII, collectively suggesting an increasing contribution from the Precordillera and Frontal Cordillera to the west (Ciccioli et al., 2014a).

In summary, the main source of sediment to DSI and II appears to be from the Toro Negro Range to the north with a growing contribution from the Precordillera and/or Frontal Cordillera by the middle/late DSII and DSIII.

4. Methods

Field samples for U-Pb dating were placed in the stratigraphic context of Ciccioli et al. (2014a) using GPS coordinates combined with original field notes and imagery. U-Pb dating was applied to tephra for stratigraphic age determination and to detrital samples for provenance analysis. Detrital zircon samples were collected from 8 freshly exposed roadcuts exposing medium-grained sandstone to pebble conglomerate deposits along the La Troya section (Table S1). Bulk material was exhumed, hand crushed, and sieved to <500 μm in the field. Eight volcanic ash samples were collected as intact fragments in the field and crushed in the lab. In the lab, all samples were wet sieved to <210 μm, rinsed to remove clay-sized particles, and zircons were separated following standard magnetic and heavy liquid procedures. Zircons were then mounted in epoxy, and polished parallel to the c-axis for analysis by laser ablation – inductively coupled plasma mass spectrometry (LA-ICPMS).

Zircon analyses were performed at the UCSB LASS facility using a Photon Machines Analyte 193-nm excimer laser and Nu Instruments Plasma MC-ICPMS, following the methods described in Kylander-Clark et al. (2013). Analyses targeted the rims of zircons free of cracks or inclusions using a spot size of 30 μm and a repetition rate of 4 Hz. Results were standardized using the 91,500 zircon reference material (Wiedenbeck et al., 1995). Standards GJ1 (601.7 ± 1.3 Ma; Jackson et al., 2004) and Plesovice (337 ± 0.37 Ma: Sláma et al., 2008) were used for secondary quality control, yielding mean $^{206}Pb/^{238}U$ ages of 599.3 ± 4.5 (n = 22; MSWD = 1.4) and337.9 ± 3.6 Ma (n = 27; MSWD = 1.1).

All tephra ages are based on $^{206}Pb/^{238}U$ ages corrected for initial Pb and secular disequilibrium. Most analyses are slightly discordant, which we attribute to minor amounts of common Pb (Fig. S1; Table S2). We correct for this by assuming concordance, calculating a 207-corrected $^{206}Pb/^{238}U$ age using ISOPLOT (Ludwig, 1991), and assuming a common $^{207}Pb/^{206}Pb$ ratio of 0.84(Stacey and Kramers, 1975). The magnitude of this age correction varies by sample, with a few grains reaching up to 50% (e.g. ash 7), but for the majority of ages, corrections are only a few percent (Fig. S1). A second correction accounts for the exclusion of ^{230}Th during crystallization, causing a period of disequilibrium in the ^{238}U-^{206}Pb decay series and a resultant age underestimate. This correction follows Schaerer (1984) as described in Schoene (2013) and assumes a Th/U ratio of 3.2 based on an average value of Mio-Pliocene ignimbrites in the Incapillo region (Fig. 1B).

For detrital zircons, cores of crack-free zircons were targeted using a spot size of 15 μm and were ablated at a rate of 4 Hz. Given the increasing possibility of Pb loss with age, 207-corrected $^{238}U/^{206}Pb$ ages are used for <1200 Ma grains, and $^{207}Pb/^{206}Pb$ ages are used for >1200 Ma. Grains that showed greater than 15% discordance between $^{238}U/^{206}Pb$ and $^{235}U/^{207}Pb$ ages were rejected, except for grains <100 Ma, which were all utilized. Detrital zircon results are displayed using kernel density estimate (KDE) plots with smoothing kernels of 0.5 Ma for ages < 50 Ma and of 4 Ma for ages > 50 Ma.

5. Discussion

5.1. Tephra ages and the pace of sedimentation

Tephra ages for the Toro Negro Formation range from 6.87 to 2.37 Ma (Fig. 4 and Table S2), indicating that sedimentation took place from Messinian (Late Miocene) to Gelasian (earliest Pleistocene) times. Each of the eight tephra beds yielded a distribution of U-Pb zircon ages reflecting differing degrees of contamination by zircons derived from pre-eruption country rock and reworking (Table S2). We assign eruptive ages based on the weighted mean age of the youngest cluster of zircons that overlap each other within 1σ uncertainty. This approach is justified by the fact that young zircons are unlikely to have experienced significant Pb loss that would lead to anomalously young ages, yet are virtually certain to have begun crystallizing hundreds of thousands of years prior to eruption (Brown and Fletcher, 1999).

The new tephra ages place constraints on the maximum duration of the basal unconformity to be < 2.4 Myr with bracketing ages of ~9.3–6.9 Ma. The DSI-DSII unconformity lies between 6.8 and 6.2 Ma, whereas the DSII-III unconformity is bracketed by ages of 5.0–3.0 Ma (Fig. 5). The basal unconformity is constrained by ash 1 located ~100 m above the unconformity, combined with a 9.34 ± 0.03 Ma ash from the Los Pozuelos section sitting ~125 m below the unconformity (Fig. 1; Ciccioli et al., 2014b). However, because up to 1000 m of the upper part of the Vinchina Formation has been eroded from the Los Pozuelos section, the actual duration of the unconformity is likely to be significantly shorter. Extrapolating the mean Vinchina sediment-accumulation rate (~0.61 mm/yr) through the existing and eroded overlying section (1125 m) suggests that the unconformity is more likely to span a time interval closer to ~7.5 to 6.9 Ma. Note that this refined age estimate is strongly dependent on the assumed sedimentation rate and the amount of eroded section lost from the upper Vinchina formation.

The DSI and II unconformity is bracketed by ash 1 and 5 (Figs. 3 and 5) and appears to have been relatively short lived based on the sedimentation rates discussed below. The DSII-DSIII unconformity is constrained by ash 9 (5.0 Ma) and the youngest grain in sample AV-10. Given that the unconformity occurs just above ash 9 and that sample AV-10 is ~300 m higher in the section, the actual depositional hiatus probably occurred shortly after ash 9: during the early Pliocene. Based on a downward extrapolation of the DSIII accumulation rate (Fig. 5), the unconformity at its base is likely to span ~1 Myr. Our data also constrain the timing of an apparent unconformity between the top of the Toro Negro Formation and the overlying Pleistocene gravels to span ~2.4–1.4 Ma. This constraint comes from the age of ash 12 and the youngest detrital zircon in sample V-25, which sits only ~20 m above it (Fig. 5).

Undecompacted sedimentation rates show striking variability: 1.2 mm/yr from ~6.9–6.1 Ma, slowing to a rate of ~0.3 mm/yr from ~6.1 to 5.0 Ma, and then accelerating back to ~0.6 mm/yr from ~3.0 to 2.4 Ma (Fig. 5). These intervals were chosen based on natural breaks in tephra-constrained sedimentation rate, which spans the DSII-III unconformity and the uppermost unconformity. Because the duration of the DSI-II unconformity is apparently quite short, we compute a long-term sedimentation rate that spans this hiatus.

The most striking implication of this revised chronology is the highly pulsed nature of deposition and erosion in the Late Miocene: prior to ~7.5 Ma, the Vinchina Formation aggraded at an average rate of ~0.61 mm/yr (Ciccioli et al., 2014b); about 1000 m of erosion occurred between 7.5 and 6.9 Ma; and then the sedimentation rate accelerated to ~1.2 mm/yr at ~6.9 Ma as deposition of the Toro

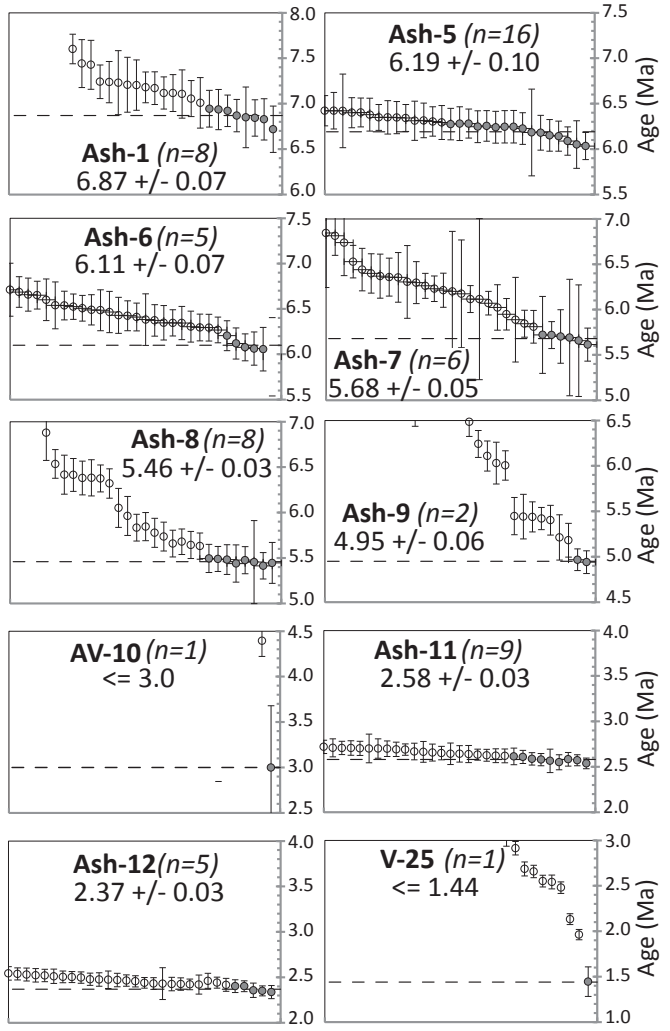

Fig. 4. Up to 30 of the youngest U-Pb zircon ages from each tephra plotted in order of descending age (2σ errors). Filled symbols denote analyses used to compute the weighted mean age, which is shown by the dashed black line. Ages are computed from the grains whose 1σ uncertainty overlaps the 1σ uncertainty of the youngest grain and are quoted with 1σ standard errors.

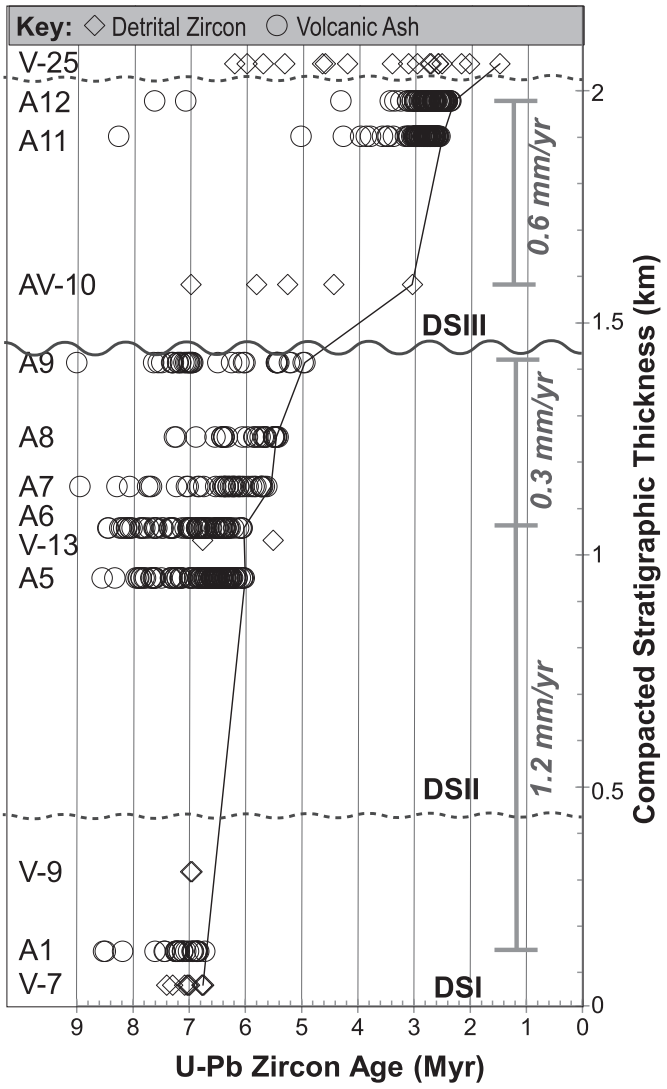

Fig. 5. U-Pb zircon grain ages shown versus stratigraphic thickness. Average compacted sedimentation rates are very high (~1.2 mm/yr) from 6.9 to 6.1 Ma, before slowing abruptly between 6.1 and 4.95 Ma (~0.3 mm/yr). Compared to overall sedimentation rates, the data suggest a relatively long unconformity (likely >1 Myr) between DSII and DSIII, but a relatively short unconformity between DSI and DSII.

Negro Formation began (Fig. 5). This succession of changes implies that between 7.5 and 6.9 Ma, the area experienced a drop in relative base level that triggered significant erosion and was then followed by a period of rapid subsidence (or basin isolation) that caused rapid sedimentation from ~6.9–6.1 Ma.

The timing of the Toro Negro basal unconformity is very similar to an unconformity observed between the Santo Domingo and El Durazno Formations in syn-orogenic strata of the eastern flank of the Sierra del Famatina ~50 km to the east (Avila). This synchrony suggests that the two events may be genetically linked: for example, by uplift along basement thrusts and/or motion on basement lineaments that uplifted the Sierra del Famatina. In this regard, Limarino et al. (2010) proposed that uplift of the Sierra Famatina produced accelerated subsidence and increased accommodation in areas proximal to the Sierra de Famatina, thus driving incision of the Vinchina Formation sitting upstream of the subsidence. During post-tectonic times, subsidence and accommodation rates proximal to the Sierra Famatina decreased (Limarino et al., 2010), triggering renewed aggradation and a return to basin filling conditions in the Toro Negro region.

Uplift in the Famatina and/or Vinchina regions at this time (roughly 7.5–6.9 Ma) is consistent with coeval uplift of isolated basement blocks elsewhere in the Bermejo Basin. Jordan et al. (2001) proposed that the Bermejo Basin transitioned from a simple to a broken foreland at ~ 7.3 Ma: a transition that is interpreted to signal activation of basement structures, such as the northern Valle Fértil Lineament. In addition, Coughlin et al. (1998) showed that exhumation in the Sierra de Valle Fértil likely began at about the same time, between 10 and 5 Ma. However, other basement blocks were uplifted earlier in the Miocene. For example, the Vinchina basin was already receiving sediments from the Toro Negro basement uplift as early as 15 Ma (Marenssi et al., 2015) and the Sierra de Famatina to the east had already experienced uplift during the early and middle Miocene (Dávila and Astini, 2007). It is thus conceivable that the deep localized incision of the Vinchina formation (the basal unconformity) was driven by uplift along basement structures in the immediate vicinity of the Vinchina basin.

The early Pliocene (shortly after 5 Ma) timing of the DSII-III unconformity is also coincident with regional tectonism. Johnson et al. (1986) infer an eastward jump in Sierra de Huaco deformation (San Juan province) at 4.8 Ma, similar in timing to a major

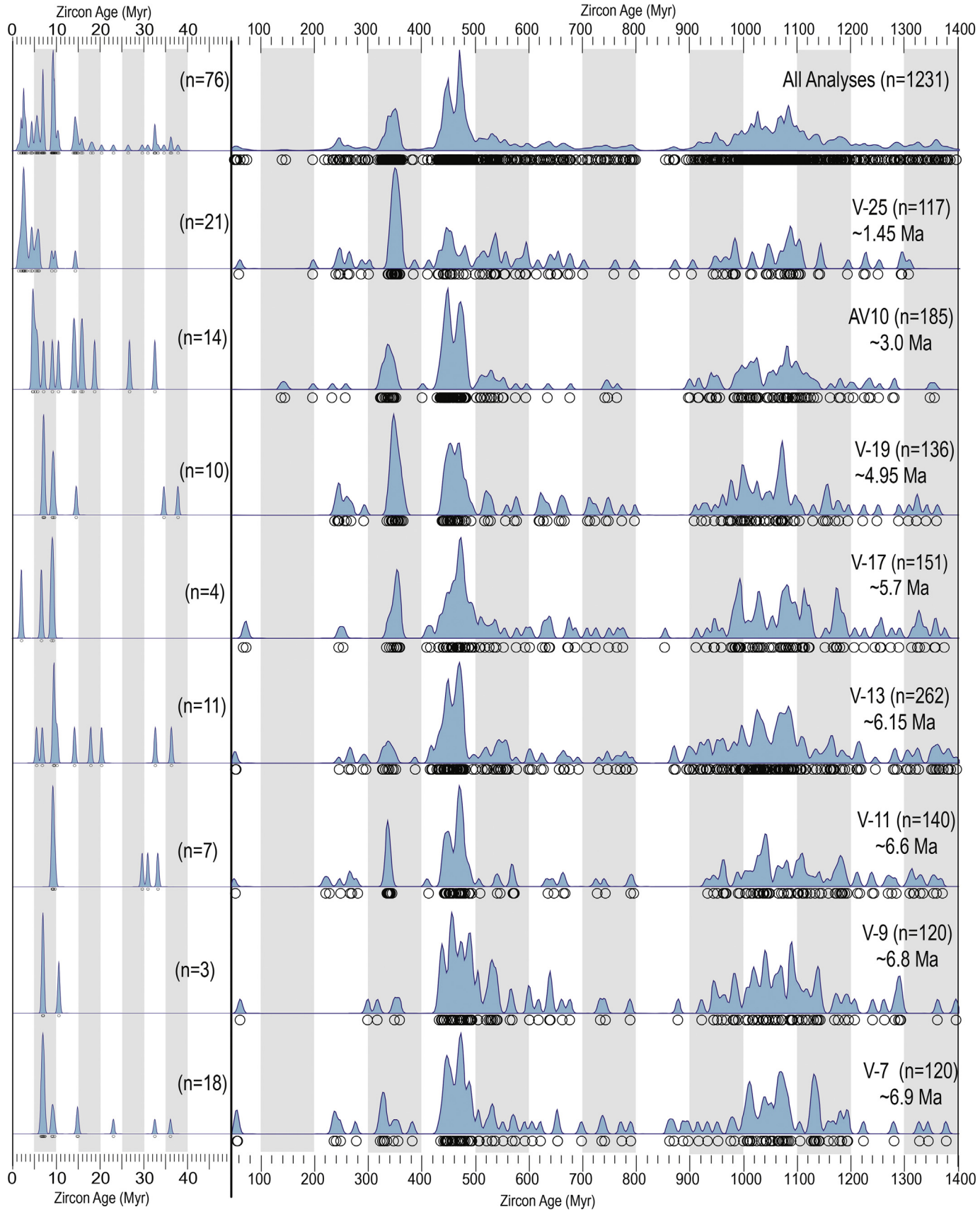

Fig. 6. Detrital U-Pb zircon spectra shown as kernel density estimates using a 4-Myr smoothing kernel for ages >50 Ma and a 0.5-Myr smoothing kernel for ages <50 Ma. Open circles represent individual grain ages (with no uncertainties).

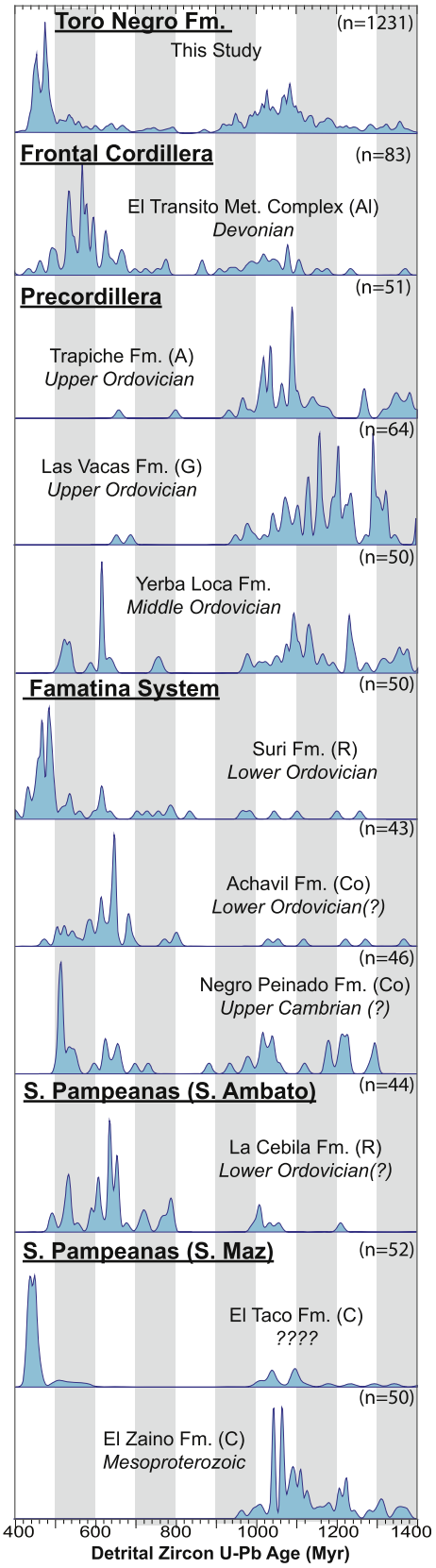

(A) = Abre et al., 2012
(Al)= Alvarez et al. 2011
(G) = Gleason et al., 2007
(C) = Casquet et al., 2008
(Co)= Collo et al., 2009*
(R) = Rapela et al. 2007

*Only $^{206}Pb/^{238}U$ ages provided

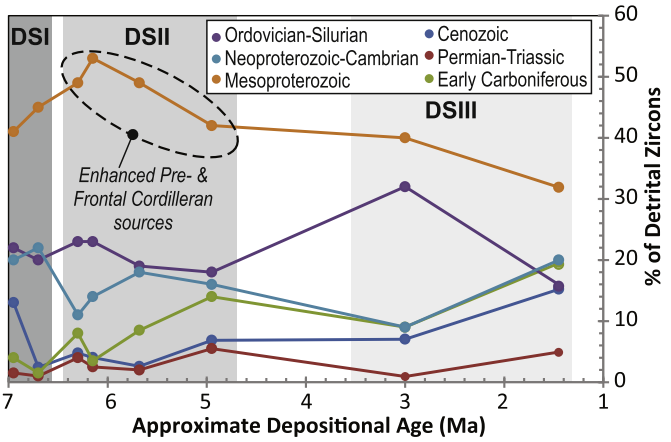

Fig. 8. The percentage of detrital zircons falling into each of the time intervals described in the text. DSII has higher proportions of Mesoproterozoic, Carboniferous, and Permian-Triassic zircons than DSI, consistent with an increase in sediment derived from the Precordillera and Frontal Cordillera to the west.

period of deformation from ~5.3 to 4.0 Ma in the Fiambalá basin about 100 km to the north (Carrapa et al., 2008).

5.2. Attribution of U-Pb age peaks

U-Pb age distributions of detrital zircons contain an impressive range of U-Pb ages, which are consistent with the expected contributions from regional bedrock units based on previous studies (Abre et al., 2012; Álvarez et al., 2011; Gleason et al., 2007; Casquet et al., 2008; Collo et al., 2009; and Rapela et al., 2007 (Figs. 6 and 7; Table S3). Here we identify seven age intervals and discuss their possible source regions. These intervals are loosely based on the major stages of geologic evolution described in Section 2 and in some cases are representative of specific source regions, but a given source more commonly contains ages from multiple age intervals. Despite recognition that zircons can also be sourced from recycled Neogene or older strata, our provenance attribution considers only direct bedrock sources.

First, Mesoproterozoic ages from (~1400-900 Ma) are the largest population, constituting ~25–50% of grains in each sample (Figs. 8 and 9). Grains of this age are dominant in the spectra of Grenville-aged basement rocks of the Western Sierras Pampeanas, e.g., the El Zaino Fm., as well as in sedimentary units of the Precordillera and the Frontal Cordillera (Fig. 7). Interestingly this population is only weakly expressed in the Cambro-Ordovician units of the Famatina System (Rapela et al., 2007; Collo et al., 2009). This minor population is consistent with the idea that these units were deposited prior to the arrival of the Precordilleran terrane(s), which are rich in Proterozoic zircons.

Second, Neoproterozoic-Cambrian ages (~900-490 Ma) represent about 10–22% of grains in each sample (Fig. 9). This population is important in the spectra of the Frontal Cordillera (El Transito Complex) and the Famatina System (Suri, Achavil, and Negro Peinado Formations), but more weakly expressed in the Precordillera and Western Sierras Pampeanas (Fig. 7).

Third, Ordovician-Silurian ages (~490-415 Ma) are also common, constituting roughly 14–34% of grains in a sample (Figs. 8 and 9).

Fig. 7. Compilation of detrital U-Pb zircon ages from bedrock units within ~200 km of the study area. Although the El Taco Formation has been interpreted as Neoproterozoic, its detrital zircon spectra suggests this unit was deposited in the Middle to Late Paleozoic.

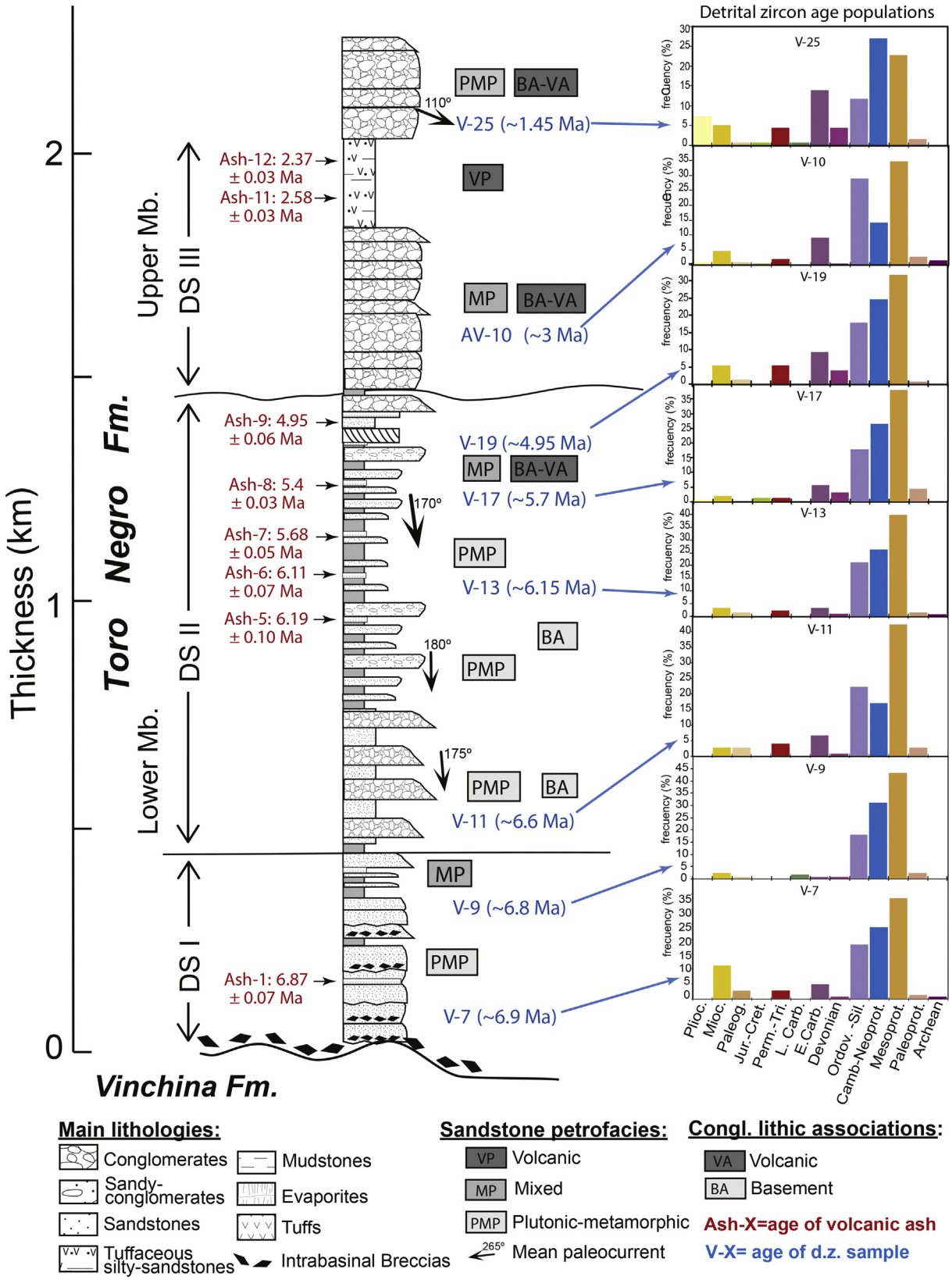

Fig. 9. Stratigraphic column showing volcanic ages from tephras, detrital zircon spectra, sandstone petrofacies, and lithic associations of conglomerates of the Toro Negro Formation in La Troya section. Bar graphs show the percentage of zircons in a given sample derived from each age interval.

This population is mostly present in the younger metasediments of the Famatina System and the Frontal Cordillera, yet is by definition absent from older Grenville-aged basement rocks of the Western Sierras Pampeanas (Fig. 7). Although we do not have spectra for the Middle-Late Paleozoic (Silurian-Permian) units exposed immediately west of the study area (Precordillera), it is likely that those

rocks are also rich in this population, because they sourced sediments from the eroding Famatinian arc. Of course, zircons of this age can also be sourced directly from granitoids currently exposed in the Famatina System, although our methods do not allow discrimination of first-vs. second-cycle zircons.

The remaining four age intervals represent minor, but persistent components of the zircon spectra (Figs. 8 and 9). They are all <360 Ma and, thus, can only be sourced from the western part of the study area. Early Carboniferous zircons (~360–320 Ma) are sourced from the Carboniferous-Permian strata directly north and west of the study area, which includes numerous volcanogenic intervals from ~348 to 340 Ma (Fig. 1). Permian -Triassic ages (~305-238 Ma) are a minor, yet persistent component that can only be sourced from western batholiths, such as the Colangüil Batholith or Montosa-El Potro complex (Fig. 1B) and probably from Del Peñón-Santo Domingo area(Caminos, 1972; Caminos et al., 1979; Coughlin, 2000). Likewise, Cretaceous-Paleocene ages (~75-55 Ma) can only be sourced from volcanic rocks exposed near the crest of the Frontal Cordillera and the western part of Precordillera (Santo Domingo area; Caminos et al., 1979). Finally, Late Cenozoic ages from ~38 to 1 Ma are sourced from the northwestern part of the study area, where they are widely exposed today (Goss et al., 2013; Kay et al., 2013).

5.3. Changes in U-Pb spectra over time

Based on the persistent presence of the <360-Ma age populations described above, a major conclusion is that the Toro Negro Formation had a continuous source of sediment from the north and west. This provenance determination supports the conclusions of Ciccioli et al. (2014a) that sediments were primarily derived from the Toro Negro Range and Frontal Cordillera-Precordillera (Fig. 1). No age populations in the zircon spectra require a sediment supply from the east or south, although they do not preclude contributions from these areas given strongly overlapping age spectra between the source regions. Although all spectra have important Ordovician-Silurian "Famatinian" peaks, it is likely that these peaks are derived from the ubiquitous Silurian-Ordovician meta-sedimentary and Late Paleozoic sedimentary units to the north and west of the basin. A second conclusion is that the first-order lithologic makeup of the source area has remained relatively constant over time. There are few major changes in the zircon spectra that require the addition or subtraction of unique source areas, although this consistency does not preclude the growth and erosion of thrust sheets or basement blocks.

Despite the lack of major changes, subtle shifts in the proportions of age populations (Figs. 6 and 8) support the idea of an increasing contribution from the Precordillera and Frontal Cordillera (Fig. 1A) during DSII and III. For example, DSI (samples V7 and V9) is distinguished from DSII (V11-V17) by relatively smaller proportions of Mesoproterozoic, Early Carboniferous, and Permo-Triassic zircons, which have important sources in the Precordillera and Frontal Cordillera to the west (Martina et al., 2011). Interestingly, the Early Carboniferous age peak seems to get systematically older with time, perhaps recording the progressive erosional unroofing of a volcaniclastic succession spanning roughly 325–355 Ma in age. Several unique Cambrian age peaks in DSI (V7-V9) from 490 to 535 Ma are not found in younger DSII or III samples; although their source is unclear, they probably come from the Toro Negro region to the north. Similar ages were obtained by Grissom et al. (1998) for a mafic – ultramafic complex in the Fiambalá range. Likewise, the DSII spectra contain a unique "shoulder" of Latest Silurian to Earliest Devonian zircons (~420-406 Ma), whose origin is unclear, but are likely associated with the Paleozoic strata of the northern Precordillera, e.g., the Punilla and Jagüé formations.

6. Conclusions

This study presents new U-Pb zircon ages on volcanic tephra that constrain the duration of previously described unconformities in the Toro Negro Formation of NW Argentina. The basal unconformity likely occurred during the latter portion of an interval spanning a 9.4–6.9 Ma (Late Miocene) window, followed by a period of very rapid sedimentation rates (~1.2 mm/yr) from 6.9 to 6.1 Ma, which occurred as the Toro Negro sediments rapidly filled paleo-valleys carved in the underlying Vinchina Formation. The basal unconformity is synchronous with an unconformity in syn-orogenic strata of the Sierra de Famatina about 50 km to the east, suggesting they may record a common tectonic forcing mechanism, such as reactivation of regional basement structures. In contrast, the DSI-II unconformity occurred between ~6.9 and 6.2 Ma and must have been short lived based on the extremely rapid sedimentation rate through this interval. Sedimentation rates then dropped nearly 5 fold to ~0.3 mm/yr from ~6.1 to 5.0 Ma, followed by the DSII-III unconformity, which occurred during the earlier portion of the 5.0–3.0 Ma (Early Pliocene) window and likely spans ~1 Myr. The uppermost Toro Negro Formation accumulated rapidly (~0.6 mm/yr) and is capped by Pleistocene gravels. These units are separated by an unconformity whose age lies between ~2.4 and 1.4 Ma.

Detrital U-Pb zircon ages from the Toro Negro Formation reveal a diverse combination of age populations consistent with the wide range of source rocks exposed in the region. The detrital zircon spectra support previous observations that sediments are primarily derived from the north and west, and that there are no major changes in sediment provenance within the entire Toro Negro Formation. Slight increases in Mesozoic, Permo-Triassic, Devonian and Carboniferous age populations are consistent with enhanced contributions from the west (Frontal Cordillera and Precordillera) during latest Miocene to earliest Pleistocene deposition (DSII and DSIII).

Acknowledgments

This research was supported by grants from the National Science Foundation (EAR-1148233, 1148268) as well as Argentine grants: UBACyT GC-385BA (Universidad de Buenos Aires), PICT 727/12, PICT 1963/14 (ANPCyT) and PIP 252 (CONICET). Thanks to Drew Gorin, Perri Silverhart, and Louise McCarren for field, lab, and nutritional assistance.

Appendix A. Supplementary data

Supplementary data related to this article can be found at http://dx.doi.org/10.1016/j.jsames.2016.05.013.

References

Abre, P., Cingolani, C.A., Cairncross, B., Chemale Jr., F., 2012. Siliciclastic Ordovician to Silurian units of the Argentine Precordillera; constraints on provenance and tectonic setting in the proto-Andean margin of Gondwana. J. S. Am. Earth Sci. 40, 1–22.

Aceñolaza, F.G., Toselli, A.J., 1981. The precambrian-lower cambrian formations of northwestern Argentina. Open-File report – U.S. Geol. Surv. 1–4.

Aceñolaza, G.F., Tortello, M.F., Esteban, S.B., 1996. Oxygen deficient facies of lower Paleozoic age in northwestern Argentina. Correlación Geol. 12, 15–21.

Álvarez, J., Mpodozis, C., Arriagada, C., Astini, R., Morata, D., Salazar, E., Valencia, V., Vervoort, J., 2011. Detrital zircons from late Paleozoic accretionary complexes in north-central Chile (28–32 deg S): possible fingerprints of the Chilenia terrane. J. S. Am. Earth Sci. 32, 460–476.

Amorosi, A., Zuffa, G.G., 2011. Sand composition changes across key boundaries of

siliciclastic and hybrid depositional sequences. Sediment. Geol. 236 (1–2), 153–163.
Astini, R.A., Marengo, L., Rubinstein, C.V., 2003. The Ordovician stratigraphy of the Sierras Subandinas (Subandean Ranges) in northwest Argentina and its bearing on an integrated foreland basin model for the Ordovician of the Central Andean region. Ser. Correlación Geol. 17, 381–386.
Bahlburg, H., Herve, F., 1997. Geodynamic evolution and tectonostratigraphic terranes of northwestern Argentina and northern Chile. Geol. Soc. Am. Bull. 109 (7), 869–884.
Beer, J.A., Jordan, T.E., 1989. The effects of Neogene thrusting on deposition in the Bermejo Basin, Argentina. J. Sediment. Petrology 59 (2), 330–345.
Borrello, A.V., Cuerda, A.J., 1967. Sobre la evolución estructural del geosinclinal paleozoico de la Precordillera, tramo montañoso Jejenes-Jáchal, provincia de San Juan. Revista del Museo de La Plata. Sección Geol. 6 (43), 111–124.
Brown, S.J.A., Fletcher, I.R., 1999. SHRIMP U-Pb dating of the preeruption growth history of zircons from the 340 ka Whakamaru Ignimbrite, New Zealand: evidence for >250 k.y. magma residence times. Geology 27 (11), 1035–1038.
Caminos, R., 1972. Upper paleozoic sedimentation and magmatism in the Cordillera frontal, Argentina. An. Acad. Bras. Ciencias 44S, 77–86.
Caminos, R. y, Fauqué, L., 2001. Hoja geológica 2969-II, Tinogasta. Provincias de La Rioja y Catamarca. Instituto de Geología y Recursos Minerales, Boletín, 276. Servicio Geológico Minero Argentino, Buenos Aires.
Caminos, R., Castellanos, T.G., Sersic, J.L., Amuchastegui, S., Caputto, R., Cocucci, A.E., Fuchs, G.L., Gordillo, C.E., Melo, C.R., 1979. Cordillera Frontal. Academia Nacional de Ciencias, Córdoba.
Caminos, R., Zamuner, A.B., Limarino, C.O., Fauqué, L., 1995. El Triásico superior fosilífero en la Precordillera riojana. Rev. la Asoc. Geol. Argent. 50, 262–265.
Carrapa, B., Hauer, J., Schoenbohm, L., Strecker, M.R., Schmitt, A.K., Villanueva, A., Sosa Gómez, J., 2008. Dynamics of deformation and sedimentation in the northern sierras Pampeanas; an integrated study of the Neogene fiambala basin, NW Argentina. Geol. Soc. Am. Bull. 120 (11–12), 1518–1543.
Caselli, A.T., Limarino, C.O., 2002. Sedimentología y evolución paleoambiental de la Formación Patquía (Pérmico) en el extremo sur de la Sierra de Maz y Cerro Bola, provincia de La Rioja, Argentina. Rev. la Asoc. Geol. Argent. 57 (4), 415–436.
Casquet, C., Pankhurst, R.J., Galindo, C., Rapela, C., Fanning, C.M., Baldo, E., Dahlquist, J., Gonzales-Casado, J.M., Colombo, F., 2008. A deformed alkaline igneous rock carbonatite complex from the western Sierras Pampeanas, Argentina; evidence for late Neoproterozoic opening of the Clymene Ocean? Precambrian Res. 165 (3–4), 205–220.
Ciccioli, P.L., 2008. Evolución paleoambiental, estratigrafía y petrología sedimentaria de la Formación Toro Negro (Neógeno), Sierras Pampeanas Noroccidentales (Provincia de La Rioja). Facultad de Ciencias Exactas y Naturales. Universidad de Buenos Aires, Argentina. Ph.D. Thesis.
Ciccioli, P.L., Marenssi, S.A., 2012. Paleoambientes sedimentarios de la Formación Toro Negro (Neógeno), antepaís fracturado andino, noroeste argentino. Andean Geol. 39 (3), 406–440.
Ciccioli, P.L., Limarino, C.O., Marenssi, S.A., 2005. Nuevas edades radimétricas para la Formación Toro Negro en la Sierra de Los Colorados, Sierras Pampeanas Noroccidentales, provincia de La Rioja. Rev. la Asoc. Geol. Argent. 60, 251–254.
Ciccioli, P.L., Limarino, C.O., Marenssi, S.A., Tedesco, A.M., Tripaldi, A., 2011. Tectosedimentary evolution of the La troya-Vinchina depocenters (northern Bermejo basin, tertiary), La Rioja province, Argentina. In: Salfity, J.A., Marquillas, R.A. (Eds.), Cenozoic Geology of the Central Andes of Argentina, SCS Publisher, Salta, pp. 91–110.
Ciccioli, P.L., Marenssi, S.A., Rossello, E., Limarino, C.O., 2013a. Sedimentary patterns in the Vinchina Basin: interplay between compressional and transcurrent tectonism during the Andean Orogeny. Bollettino di Geofisica teorica ed applicata 54 Supplement 2, pp. 217–220.
Ciccioli, P.L., Gómez O'Connell, M., Limarino, C.O., Marenssi, S.A., 2013b. La sucesión terciaria de la quebrada de Los Pozuelos (Cuenca de Vinchina): su importancia estratigráfica y paleogeográfica para el antepaís andino. Rev. la Asoc. Geol. Argent. 70 (4), 451–464.
Ciccioli, P.L., Marenssi, S.A., Limarino, C.O., 2014a. Petrology and provenance of the Toro Negro Formation (Neogene) of the Vinchina broken foreland basin (central Andes of Argentina). J. S. Am. Earth Sci. 49, 15–38.
Ciccioli, P.L., Limarino, C.O., Friedman, R., Marenssi, S.A., 2014b. New high precision U-Pb ages for the Vinchina formation: implications for the stratigraphy of the Bermejo andean foreland basin (La Rioja province, Western Argentina). J. S. Am. Earth Sci. 56, 200–213.
Cobbold, P.R., Davy, P., Gapais, D., Rossello, E.A., Sadybakasov, E., Thomas, J.C., Tondji Biyo, J.J., de Urreiztieta, M., 1993. Sedimentary basins and crustal thickening. Sediment. Geol. 86 (1–2), 77–89.
Collo, G., Astini, R.A., Cawood, P.A., Buchan, C., Pimentel, M., 2009. U-Pb detrital zircon ages and Sm-Nd isotopic features in low-grade metasedimentary rocks of the Famatina Belt; implications for late Neoproterozoic-early Palaeozoic evolution of the proto-Andean margin of Gondwana. J. Geol. Soc. Lond. 166 (2), 303–319.
Collo, G., Dávila, F.M., Nóbile, J., Astini, R.A., Gehrels, G., 2011. Clay mineralogy and thermal history of the Neogene Vinchina Basin, central Andes of Argentina: analysis of factors controlling the heating conditions. Tectonics 30 (4), TC4012. http://dx.doi.org/10.1029/2010TC002841.
Colombo, F., Baldo, E.G.A., Casquet, C., Pankhurst, R.J., Galindo, C., Rapela, C.W., Dahlquist, J.A., Fanning, C.M., 2009. A-type magmatism in the sierras of Maz and Espinal; a new record of Rodinia breakup in the western Sierras Pampeanas of Argentina. Precambrian Res. 175 (1–4), 77–86.
Coughlin, T.J., 2000. Linked Orogen-oblique Fault Zones in the Central Argentine Andes; the Basis of a New Model for Andean Orogenesis and Metallogenesis. University of Queensland. Ph.D. thesis.
Coughlin, T.J., O'Sullivan, P.B., Kohn, B.P., Holcombe, R.J., 1998. Apatite fission-track thermochronology of the Sierras Pampeanas, central western Argentina: implications for the mechanism of plateau uplift in the Andes. Geology 26 (11), 999–1002.
Dahlquist, J.A., Alasino, P.H., Galindo, C., Pankhurst, R.J., Rapela, C.W., Saavedra, J., Casquet, C., Baldo, E.G., Gonzalez Casado, J.M., 2006. Evolución magmática del Granito Peñón Rosado, Cerro Asperecito, flanco occidental de la sierra de Famatina. Rev. la Asoc. Geol. Argent. 61 (1), 93–111.
Dávila, F.M., Astini, R.A., 2007. Cenozoic provenance history of synorogenic conglomerates in western Argentina (Famatina Belt); implications for central Andean foreland development. Geol. Soc. Am. Bull. 119 (5–6), 609–622.
de la Fuente, M.S., Ciccioli, P.L., Limarino, C.O., Gutiérrez, P.R., Fauque, L.E., 2003. Quelonios podocnemididos en la Formación Puesto La Flecha (Oligoceno), Precordillera de La Rioja, Argentina. Ameghiniana 40 (4), 617–624.
Dickinson, W.R., Suczek, C.A., 1979. Plate tectonics and sandstone compositions. AAPG Bull. 63 (12), 2164–2182.
Espejo, I.S., López-Gamundí, O.R., 1994. Source versus depositional controls on sandstone composition in a foreland basin; the el imperial formation (mid carboniferous-lower permian), san rafael basin, western Argentina. J. Sediment. Res. Sect. A Sediment. Petrology Process. 64 (1), 8–16.
Gleason, J.D., Finney, S.C., Peralta, S.H., Gehrels, G.E., Marsaglia, K.M., 2007. Zircon and whole-rock Nd-Pb isotopic provenance of middle and upper ordovician siliciclastic rocks, Argentine Precordillera. Sedimentology 54 (1), 107–136.
Goss, A.R., Kay, S.M., Mpodozis, C., 2013. Andean adakite-like high-Mg andesites on the northern margin of the Chilean-Pampean flat-slab (27–28.5° S) associated with frontal arc migration and fore-arc subduction erosion. J. Petrol. 54 (11), 2193–2234.
Grissom, G.C., Debari, S.M., Snee, L.W., 1998. Geology of the Sierra de Fiambala, northwestern Argentina; implications for early Palaeozoic Andean tectonics. Geol. Soc. Spec. Publ. 142, 297–323.
Grosse, P., Soellner, F., Baez, M.A., Toselli, A.J., Rossi, J.N., de la Rosa, J.D., 2009. Lower Carboniferous post-orogenic granites in central-eastern Sierra de Velasco, Sierras Pampeanas, Argentina; U-Pb monazite geochronology, geochemistry and Sr-Nd isotopes. Int. J. Earth Sci. 98 (5), 1001–1025.
Gulbranson, E.L., Montañez, I.P., Schmitz, M.D., Limarino, C.O., Isbell, J.L., Marenssi, S.A., Crowley, J.L., 2010. High-precision U-Pb calibration of Carboniferous glaciation and climate history, Paganzo Group, NW Argentina. Bull. Geol. Soc. Am. 122 (9–10), 1480–1498.
Gulbranson, E.L., Montañez, I.P., Tabor, N.J., Limarino, C.O., 2015. Late Pennsylvanian aridification on the southwestern margin of Gondwana (Paganzo Basin, NW Argentina); a regional expression of a global climate perturbation. Palaeogeogr. Palaeoclimatol. Palaeoecol. 417, 220–235.
Henry, L.C., Isbell, J.L., Limarino, C.O., 2008. Carboniferous glacigenic deposits of the proto-Precordillera of west-central Argentina. Special Pap. Geol. Soc. Am. 441, 131–142.
Jackson, S.E., Pearson, N.J., Griffin, W.L., Belousova, E.A., 2004. The application of laser ablation-inductively coupled plasma-mass spectrometry to in situ U-Pb zircon geochronology. Chem. Geol. 211 (1–2), 47–69.
Johnson, N.M., Jordan, T.E., Johnsson, P.A., Naeser, C.W., 1986. Magnetic polarity stratigraphy, age and tectonic setting of fluvial sediments in an eastern Andean foreland basin, San Juan Province, Argentina. Special Publ. Int. Assoc. Sedimentologists 8, 63–75.
Jordan, T.E., Allmendinger, R.W., Damanti, J.F., Drake, R.E., 1993. Chronology of motion in a complete thrust belt; the Precordillera, 30–31 degrees S, Andes Mountains. J. Geol. 101 (2), 135–156.
Jordan, T.E., Schlunegger, F., Cardozo, N., Gónzalez-Bonorino, G., Kraemar, P., Re, G., 2001. Unsteady and spatially variable evolution of the Neogene Andean Bermejo foreland basin, Argentina. J. S. Am. Earth Sci. 14 (7), 775–798.
Kay, S.M., Abbruzzi, J.M., 1996. Magmatic evidence for Neogene lithospheric evolution of the central Andean "flat-slab" between 30° S and 32° S. Tectonophysics 259 (1–3), 15–28.
Kay, S.M., Maksaev, V., Moscoso, R., Mpodozis, C., Nasi, C., 1987. Probing the evolving Andean lithosphere; mid-late Tertiary magmatism in Chile (29°–30° 30') over the modern zone of subhorizontal subduction. J. Geophys. Res. 92 (B7), 6173–6189.
Kay, S.M., Mpodozis, C., Gardeweg, M., 2013. Magma sources and tectonic setting of Central Andean andesites (25.5-28° S) related to crustal thickening, forearc subduction erosion and delamination. Special Publ. Geol. Soc. Lond. 385 (1), 303–334.
Kilmurray, J.O., 1971. Las ortoanfibolitas de la Sierra de Maz, Provincia de La Rioja. Revista del Museo de La Plata. Secc. Geol. 7 (55), 51–75.
Kylander-Clark, A.R.C., Hacker, B.R., Cottle, J.M., 2013. Laser ablation split stream ICP petrochronology. Chem. Geol. 345, 99–112.
Limarino, C.O., Tripaldi, A., Marenssi, S.A., Net, L.I., Re, G., Caselli, A.T., 2001. Tectonic control on the evolution of the fluvial systems of the VinchinaFormation (Miocene), Northwestern Argentina. J. S. Am. Earth Sci. 14 (7), 751–762.
Limarino, C.O., Fauqué, L., Ciccioli, P.L., Tedesco, A.M., Marsicano, C., Arcucci, 2005. El Mesozoico De La Precordillera Septentrional. In: 15th Congreso Geológico Argentino, La Plata, I, pp. 217–222.
Limarino, C.O., Tripaldi, A., Marenssi, S.A., Fauque, L., 2006. Tectonic, sea-level, and climatic controls on late Paleozoic sedimentation in the western basins of Argentina. J. S. Am. Earth Sci. 22 (3–4), 205–226.

Limarino, C.O., Ciccioli, P.L., Marenssi, S.A., 2010. Análisis del contacto entre las formaciones Vinchina y Toro Negro (Sierra de Los Colorados, provincia de La Rioja, Argentina), sus implicancias tectonicas. Lat. Am. J. Sedimentology Basin Analysis 17 (2), 113–132.
Llambías, E.J., Sato, A.M., 1992. The colanguil batholith (29-31° S), Cordillera frontal, Argentina; structure and tectonic environment. Int. Geol. Rev. 34 (7), 687–709.
López Gamundí, O.R., 1987. Depositional models for the glaciomarine sequences of Andean late Paleozoic basins of Argentina. Sediment. Geol. 52 (1–2), 109–126.
Ludwig, K.R., 1991. ISOPLOT; a Plotting and Regression Program for Radiogenic-isotope Data; Version 2.53: Open-file Report - U. S. Geological Survey, p. 39.
Mangano, M.G., Droser, M.L., 2003. Ecospace utilization and paleoenvironmental expansion during the Ordovician radiation; the ichnologic evidence. Ser. Correlación Geol. 17, 315–319.
Marenssi, S.A., Ciccioli, P.L., Limarino, C.O., Schencman, L.J., Díaz, M.Y., 2015. Using fluvial cyclicity to decipher the interaction of basement- and fold-thrust-belt tectonics in a broken foreland basin; Vinchina Formation (Miocene), northwestern Argentina. J. Sediment. Res. 85 (4), 361–380.
Martina, F., Astini, R.A., Becker, T.P., Thomas, W.A., 2005. In: Granitos Grenvilianos milonitizados en la faja de deformación de Jagué, noroeste de La Rioja. In: 16th Congreso Geológico Argentino, La Plata, 4, pp. 591–594.
Martina, F., Viramonte, J.M., Astini, R.A., Pimentel, M.M., Dantas, E., 2011. Mississippian volcanism in the south-central Andes; new U/Pb SHRIMP zircon geochronology and whole rock geochemistry. Gondwana Res. 19 (2), 524–534.
Milana, J.P., Bercowski, F., Jordan, T., 2003. Paleoambientes y magnetoestratigrafía del Neógeno de la Sierra de Mogna, y su relación con la cuenca de antepaís andina. Rev. la Asoc. Geol. Argent. 58 (3), 447–473.
Mpodozis, C., Kay, S.M., 1992. Late paleozoic to triassic evolution of the Gondwana margin; evidence from chilean frontal cordilleran batholiths (28° S to 31° S); with suppl. Data 92–22. Geol. Soc. Am. Bull. 104 (8), 999–1014.
Mulch, A., Uba, C.E., Strecker, M.R., Schoenberg, R., Chamberlain, C.P., 2010. Late Miocene climate variability and surface elevation in the central Andes. Earth Planet. Sci. Lett. 290 (1–2), 173–182.
Nasi, P.C., Mpodozis, M.C., Cornejo, P.P., Moscoso, D.R., Maksaev, J.,V., 1985. El Batolito Elqui-Limari (Paleozoico Superior-Triásico); características petrográficas, geoquímicas y significado tectónico. Rev. Geol. Chile 25–26, 77–111.
Net, L.I., Limarino, C.O., 2006. Applying sandstone petrofacies to unravel the Upper Carboniferous evolution of the Paganzo Basin, northwest Argentina. J. S. Am. Earth Sci. 22 (3–4), 239–254.
Pankhurst, R.J., Rapela, C.W., Saavedra, J., Baldo, E., Dahlquist, J., Pascua, I., Fanning, C.M., 1998. The Famatinian magmatic arc in the central Sierras Pampeanas; an Early to Mid-Ordovician continental arc on the Gondwana margin. Geol. Soc. Spec. Publ. 142, 343–367.
Pankhurst, R.J., Rapela, C.W., Fanning, C.M., 2000. Age and origin of coeval TTG, I- and S-type granites in the Famatinian Belt of the NW Argentina. Trans. R. Soc. Edinb. Earth Sci. 91, 151–168. Parts 1–2.
Ramos, V.A., 1970. Estratigrafía y estructura del terciario en la Sierra de los Colorados (provincia de La Rioja), Republica Argentina. Rev. la Asoc. Geol. Argent. 25 (3), 359–382.
Ramos, V.A., Folguera, A., 2009. Andean flat-slab subduction through time. Geol. Soc. Spec. Publ. 327, 31–54.
Ramos, V.A., Jordan, T.E., Allmendinger, R.W., Mpodozis, C., Kay, S.M., Cortes, J.M., Palma, M., 1986. Paleozoic terranes of the central Argentine-chilean Andes. Tectonics 5 (6), 855–880.
Rapela, C.W., Heaman, L.M., McNutt, R.H., 1982. Rb-Sr geochronology of granitoid rocks from the Pampean Ranges, Argentina. J. Geol. 90 (5), 574–582.
Rapela, C.W., Pankhurst, R.J., Casquet, C., Baldo, E., Saavedra, J., Galindo, C., 1998. Early evolution of the proto-andean margin of South America. Geol. (Boulder) 26 (8), 707–710.
Rapela, C.W., Coira, B., Toselli, A.J., Llambías, E.J., 1999. In: Caminos, R. (Ed.), El basamento Precámbrico-Paleozoico inferior de las Sierras Pampeanas, Famatina, Cordillera Oriental y Puna. Sistema Famatiniano de las Sierras Pampeanas y magmatismo Eeopaleozoico de las Sierras Pampeanas, de la Cordillera Oriental y Puna. In: Geología Argentina, 29. Dirección Nacional del Servicio Geológico. Anales, Buenos Aires, pp. 145–158.
Rapela, C.W., Pankhurst, R.J., Casquet, C., Fanning, C.M., Baldo, E.G., Gonzalez-Casado, J.M., Galindo, C., Dahlquist, J., 2007. The Rio de la Plata craton and the assembly of SW Gondwana. Earth-Science Rev. 83 (1–2), 49–82.
Rapela, C.W., Pankhurst, R.J., Casquet, C., Baldo, E., Galindo, C., Fanning, C.M., Dahlquist, J.M., 2010. The western Sierras Pampeanas; protracted Grenville age history (1330-1030 Ma) of intra-oceanic arcs, subduction-accretion at continental edge and AMCG intraplate magmatism. J. S. Am. Earth Sci. 29 (1), 105–127.
Ré, G.H., Barredo, S.P., 1993. Esquema de correlación magnetoestratigráfica deformaciones terciarias aflorantes en las provincias de San Juan, aflorantes en las provincias de San Juan, La Rioja y Catamarca. Rev. la Asoc. Geol. Argent. 48 (3e4), 241–246.
Reynolds, J.H., 1987. Chronology of Neogene Tectonics in the Central Andes (27°–33°S) of Western Argentina Based on the Magnetic Polarity Stratigraphy of Foreland Basin Sediments. Dartmouth College. Ph.D. thesis.
Rossello, E.A., Mozetic, M.E., Cobbold, P.R., de Urreizttieta, M., Gapais, D., 1996. In: El espolón Umango-Maz y la conjugación sintaxial de los lineamientos Tucumán y Valle Fértil (La Rioja, Argentina). In: 13th Congreso Geológico Argentino and 3rd Congreso de Exploración de Hidrocarburos. Buenos Aires, 2, pp. 187–194.
Rubiolo, D., Cisterna, C., Villeneuve, M., Hickson, C., 2002. In: Edad U/Pb del granito de Las Angosturas en la Sierra de Narváez; Sistema de Famatina, provincia de Catamarca. In: 15th Congreso Geológico Argentino, 1, pp. 359–362.
Scalabrini Ortiz, J., 1973. In: El Carbónico de la Precordillera Argentina al norte del Río Jáchal. In: 5th Jornadas Geológicas Argentinas, 3, pp. 387–401.
Schaerer, U., 1984. The effect of initial ^{230}Th disequilibrium on young U-Pb ages; the Makalu case, Himalaya. Earth Planet. Sci. Lett. 67 (2), 191–204.
Schoene, B., 2013. U-Th-Pb geochronology. In: Holland, H.D., Turekian, K.K. (Eds.), Treatise on Geochemistry, 4. Elsevier, Oxford, pp. 341–378.
Sims, J.P., Ireland, T.R., Camacho, A., Lyons, P., Pieters, P.E., Skirrow, R.G., Stuart-Smith, P.G., Miro, R., 1998. In: U-pb, Th-pb and Ar-ar Geochronology from the Southern Sierras Pampeanas, Argentina; Implications for the Palaeozoic Tectonic Evolution of the Western Gondwana Margin, 142. Geological Society Special Publications, pp. 259–281.
Sláma, J., Košler, J., Condon, D.J., Crowley, J.L., Gerdes, A., Hanchar, J.M., Horstwood, M.S.A., Morris, G.A., Nasdala, L., Norberg, N., Schaltegger, U., Schoene, B., Tubrett, M.N., Whitehouse, M.J., 2008. Plešovice zircon — a new natural reference material for U-Pb and Hf isotopic microanalysis. Chem. Geol. 249 (1–2), 1–35.
Stacey, J.S., Kramers, J.D., 1975. Approximation of terrestrial lead isotope evolution by a 2-Stage model. Earth Planet. Sci. Lett. 26 (2), 207–221.
Strecker, M.R., Alonso, R.N., Bookhagen, B., Carrapa, B., Hilley, G.E., Sobel, E.R., Trauth, M.H., 2007. Tectonics and climate of the southern central Andes. Annu. Rev. Earth Planet. Sci. 35, 747–787.
Tabbutt, K.D., Naeser, ChW., Jordan, T.E., Cerveny, P.F., 1989. New fission-track ages of Mio-pliocene tuffs in the sierras Pampeanas and Precordillera of Argentina. Rev. la Asoc. Geol. Argent. 44 (1–4), 408–419.
Tedesco, A.M., Limarino, C.O., Ciccioli, P.L., 2007. Primera edad radimétrica de los depósitos Cretácicos de la Precordillera Central. Rev. la Asoc. Geol. Argent. 62 (3), 471–474.
Tripaldi, A., Limarino, C.O., 2005. Vallecito Formation (Miocene); the evolution of an eolian system in an Andean foreland basin (northwestern Argentina). J. S. Am. Earth Sci. 19 (3), 343–357.
Tripaldi, A., Net, L., Limarino, C., Marenssi, S., Re, G., Caselli, A., 2001. Paleoambientes sedimentarios y procedencia de la Formacion Vinchina, Mioceno, noroeste de la provincia de La Rioja. Rev. la Asoc. Geol. Argent. 56 (4), 443–465.
Turner, J.C.M., 1964. Descripción geológica de la Hoja 15c, Vinchina, provincia de La Rioja. Buenos Aires. Dirección Nac. Geol. Minería Bol. 100, 81.
Turner, J.C.M., 1967. In: Descripción geológica de la hoja 13b, Chaschuil (provincias de Catamarca y La Rioja), escala 1:200.000, 106. Instituto Nacional de Geología Minera, Boletín, p. 78.
Varela, R., Roverano, D., Sato, M.A., 2000. Granito El Peñón, Sierra de Umango; descripcion, edad Rb/Sr e implicancias geotectónicas. Rev. la Asoc. Geol. Argent. 55 (4), 407–413.
Varela, R., Basei, M.A.S., Gonzalez, P.D., Sato, A.M., Naipauer, M., Campos Neto, M., Cingolani, C.A., Meira, V.T., 2011. Accretion of Grenvillian terranes to the southwestern border of the Rio de la Plata craton, western Argentina. Int. J. Earth Sci. 100 (2–3), 243–272.
Wiedenbeck, M., Alle, P., Corfu, F., Griffin, W.L., Meier, M., Oberli, F., 1995. Three natural zircon standards for U-Th-Pb, Lu-Hf, trace element and REE analyses. Geostand. Newsl. 19, 1–23.